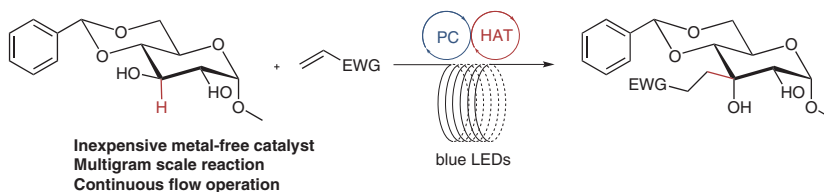


# $\alpha$ -C–H Photoalkylation of a Glucose Derivative in Continuous Flow

Marc L. M. C. Mouthaan<sup>a</sup>Kees Pouwer<sup>b</sup>Mark L. G. Borst<sup>b</sup>Martin D. Witte<sup>a</sup> Adriaan J. Minnaard<sup>\*a</sup> 

<sup>a</sup> Department of Chemical Biology, Stratingh Institute for Chemistry,  
University of Groningen, Groningen, The Netherlands  
A.J.Minnaard@RUG.nl

<sup>b</sup> Symeres B.V., Kadijk 3, 9747 AT Groningen, The Netherlands




Received: 20.03.2022

Accepted after revision: 28.04.2022

Published online: 02.05.2022

DOI: 10.1055/a-1840-5483; Art ID: ss-2022-m0141-fa

License terms: 

© 2022. The Author(s). This is an open access article published by Thieme under the terms of the Creative Commons Attribution License, permitting unrestricted use, distribution and reproduction, so long as the original work is properly cited. (<https://creativecommons.org/licenses/by/4.0/>)

**Abstract** Site-selective photoalkylation is a powerful strategy to extend the carbon framework of carbohydrates, otherwise often attainable only through laborious syntheses. This work describes the adaptation and upscaling of the photoalkylation of a glucose derivative as a continuous flow process. The reported iridium catalyst is replaced by an organic sensitizer and the reaction has been carried out on 40-gram scale.

**Key words** C–H functionalization, photoredox catalysis, carbohydrates, flow chemistry, hydrogen atom transfer, radicals

The natural abundance and diversity in stereochemistry of carbohydrates make them interesting starting materials for the development of novel pharmaceutical compounds and organic materials. The lion's share of the literature on the modification of carbohydrates in this context is focused on reactions involving the hydroxyl groups, such as ether or ester formation.<sup>1,2</sup>

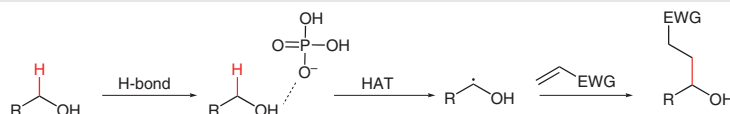
As discrimination between these multiple hydroxy groups is difficult, protecting group strategies are commonly used. An alternative approach is direct carbon–carbon bond formation, but apart from reactions with the carbonyl

group in carbohydrates (such as aldol and related reactions, and Strecker reactions) this approach is not often pursued. With the advent of synthetically attractive photoredox chemistry,<sup>3,4</sup> site-selective photoalkylation has come into play as a powerful strategy to extend the carbon framework of carbohydrates. Carbohydrates are intrinsically attractive substrates for radical-based reactions involving the carbon skeleton, because the hydroxy groups themselves are not very reactive in such a setting.<sup>5</sup> Nevertheless, the challenge of site-selectivity remains.

In 2015, the group of MacMillan made use of the fact that hydrogen bond formation between an acceptor and a hydroxy group weakens the  $\alpha$ -C–H bond strength of that hydroxy group and this leads to preferential hydrogen atom transfer (HAT).<sup>6</sup> The produced carbon-centered radical can subsequently react with an electron-deficient alkene, a 'sophophile' (Scheme 1).

This activation is sufficiently large to discriminate between  $\alpha$ -C–H bonds in ethers or acetals and a free hydroxyl group, and this was illustrated in the selective alkylation of a protected galactose derivative, possessing one hydroxy group (Scheme 2).

We subsequently showed that this photoredox alkylation reaction based on hydrogen bond based activation can also be applied on unprotected carbohydrates.<sup>7</sup> The site-selectivity in these cases is substrate inherent and the hydrogen bond formation functions to increase the reactivity (or makes the reaction possible at all). In gluco- and allopyranosides it was observed that alkylation occurs selectively at



**Scheme 1** The addition of a hydrogen bond acceptor allows for  $\alpha$ -C–H activation<sup>6</sup>

## Biographical Sketches



**Marc Mouthaan** obtained his B.Sc. and M.Sc. degrees in chemistry from the University of Groningen, working on the functionalization of carbohydrates with professor A. J.

Minnaard. Upon completing his studies, he returned to the group of prof. Minnaard in late 2019 to pursue a Ph.D. in collaboration with industry partner Symeres. His current research is

focused on employing carbohydrate derivatives as scaffolds for medicinal chemistry, as well as applying cheminformatics tools to assist organic synthesis.



**Kees Pouwer** received his PhD in 1995 in the group of professor Wynberg at the university of

Groningen. He has worked at Symeres, formerly known as Syncom, since 1997. Currently

he is director of Chemistry.



**Mark Borst** received his M.Sc. and Ph.D. studies at Vrije Universiteit Amsterdam, with professor Koop Lammertsma and

obtained his Ph.D. in 2005. Right after, he joined Syncom (now part of Symeres) in Groningen, the Netherlands, since

2013 in the role of Project Leader, with a focus on scaffold design and parallel chemistry.



**Martin D. Witte** performed his Ph.D. studies at Leiden University, The Netherlands, under the supervision of Prof. Overkleeft and Prof. van der Marel and obtained his Ph.D. in 2009. In 2010, he joined the

group of Prof. Ploegh at the Whitehead Institute for Biomedical Research, Cambridge, USA to do postdoctoral research. In 2013, he was appointed assistant professor in chemical biology at the University of

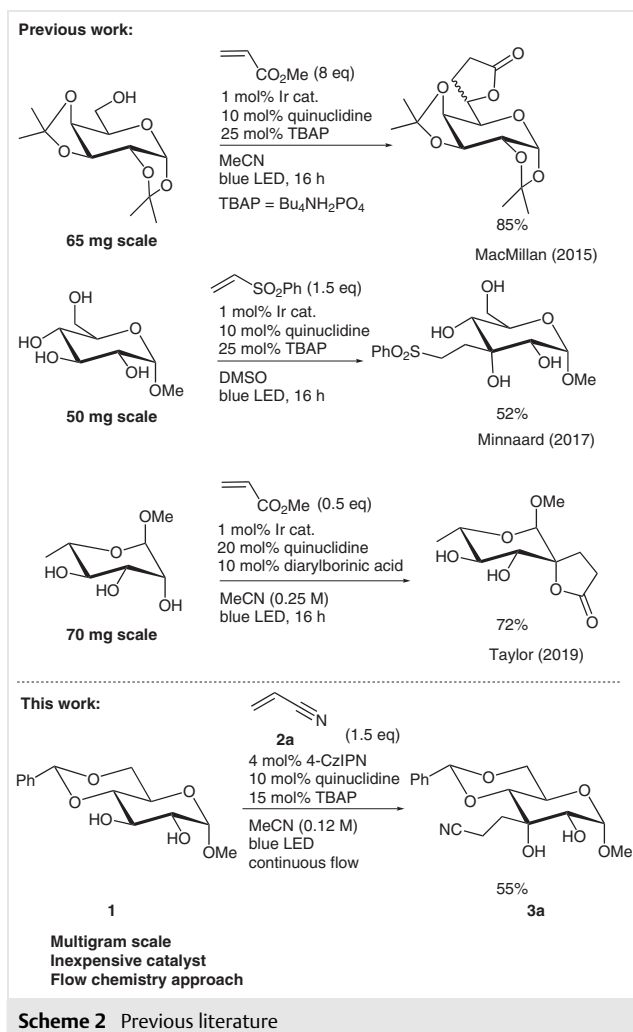
Groningen, The Netherlands and in 2018 has been promoted to associate professor. His research focuses on the site selective modification of biomolecules and the development of new protein labeling tools.



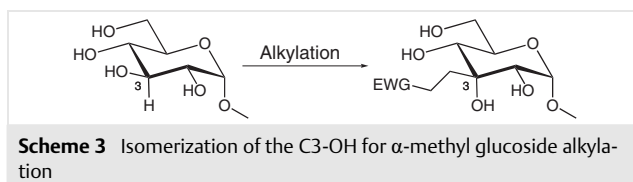
**Adriaan Minnaard** obtained his PhD at Wageningen Agricultural University, The Netherlands. He is professor in Chemical Biology at the Stratingh Institute for Chemistry,

University of Groningen, and has been director of this institute. His research interests are the synthesis and modification of complex natural products, including carbohydrates, and his

group contributes as well to the development of new synthesis methods. His research on the lipidome of *M. tuberculosis* received the NWO-TEAM Science Award 2020.



the C3 carbon (Scheme 3). Furthermore, when the  $\alpha$ -anomers of the substrates were used, alkylation took place from the top face, resulting in an *allo*-configured product. This selectivity likely originates from the steric shielding by the anomeric substituent. With  $\beta$ -methyl glucosides, only partial inversion was observed.



Next to hydrogen bond formation, several other methods have been reported, with the common theme that the electron density of the  $\alpha$ -carbon is increased. Boron, tin and silicon are less electronegative than hydrogen, so diaryl-

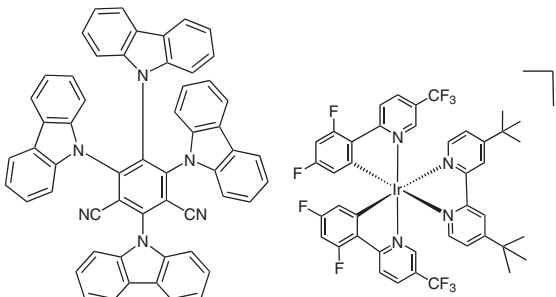
borinic acids,<sup>8</sup> borinates,<sup>9</sup> spiro-silanes<sup>10</sup> and organostannanes<sup>11</sup> have all been used successfully, and are instrumental to induce regioselectivity in the alkylation, with the latter being applied to rhamnopyranosides. Alkylation via 1,6-HAT in a fructopyranoside has been reported as well.<sup>12</sup>

Also, the nature of the hydrogen atom transfer agent has been studied, with quinuclidine being favored. Recently however, quinuclidine-<sup>13</sup> and DABCO-derived<sup>14</sup> catalysts have also proven useful for facilitating HAT. This type of photocatalysis is not limited to alkylations: in more recent reports, Wendlandt and co-workers have used the HAT reaction for isomerization, providing access to rare monosaccharides from commonly available monosaccharides,<sup>15,16</sup> whilst the group of Taylor employed the system for oxidations.<sup>17</sup> Redox isomerization, a strategy that combines the two, gives rise to ketodeoxysugars, with examples of both furanosides<sup>18</sup> and pyranosides<sup>19,20</sup> having been investigated. The photocatalytic system has also seen success in chiral resolutions: with a chiral phosphate, racemic ureas could be enantiomerically enriched.<sup>21</sup>

It is therefore clear that the versatility of these photoredox systems makes them very interesting candidates to explore otherwise challenging chemistry. Despite this progress however, the photoalkylation of carbohydrates has not yet been used to prepare building blocks or scaffolds on a preparative scale. In order to be synthetically useful, the procedure needs to be scalable and cost-effective. In addition, the variety in somophiles is still rather limited, restricting structural diversity. To improve upon this situation, we envisioned applying a continuous flow chemistry approach. One of the key advantages of continuous flow chemistry is the much larger surface area offered by the tubing. This allows for more efficient irradiation compared to a batch setup. In addition, the amount of product does not depend on the scale of the reaction but on the overall runtime.<sup>22</sup>

Since our primary goal was the upscaling of these known alkylation reactions, use of the well-studied iridium catalyst  $\text{Ir}[\text{dF}(\text{CF}_3)\text{ppy}]_2(\text{dtbbpy})\text{PF}_6$  (Table 1) was not cost-effective. Iridium prices have increased substantially in recent times and producing multigram quantities of product without being able to recycle the catalyst would be far too costly. In 2020, Wendlandt and co-workers reported on the selective epimerization of carbohydrates<sup>15</sup> by photoredox chemistry and in this study, the iridium catalyst was replaced by the organocatalyst 4-CzIPN. Given the similarity of our reaction, as well as the range of redox potentials, we hypothesized that 4-CzIPN might also be effective in our alkylation reactions. In addition to being a metal-free alternative, 4-CzIPN is prepared in a single step from readily available materials<sup>23</sup> and has greater absorption in the visible light region, which better matches the used light source.

**Table 1** Photocatalysts Used for the Reactions in this Study

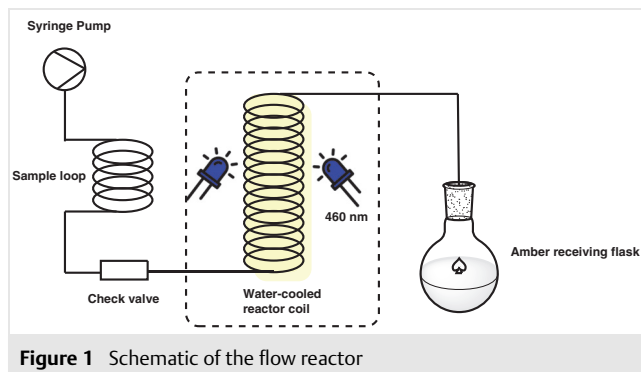
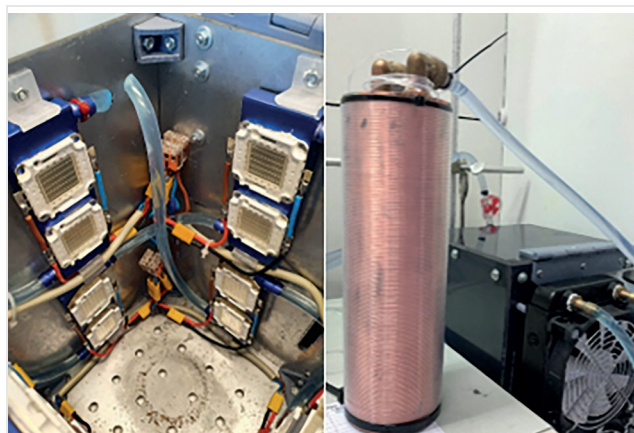
		
I	II	
4-CzIPN	Ir[dF(CF <sub>3</sub> )ppy] <sub>2</sub> (dtbbpy)PF <sub>6</sub>	<sup>+</sup> PF <sub>6</sub> <sup>−</sup>
4-CzIPN	Iridium catalyst	
Redox potentials: <sup>24</sup>		
<i>E</i> <sub>1/2</sub> (P <sup>+</sup> /P)	+1.35 V	+1.21 V
<i>E</i> <sub>1/2</sub> (P/P <sup>−</sup> )	−1.21 V	−1.37 V
λ <sub>abs</sub> (in MeCN): <sup>25</sup>	435 nm	380 nm

To facilitate workup and purification of the photoalkylated products, we chose methyl 4,6-*O*-benzylidene- $\alpha$ -D-glucopyranoside as the substrate. Although the photoalkylation reaction does not explicitly require the presence of the 4,6-*O*-benzylidene moiety, as we showed previously,<sup>7</sup> the starting material is readily prepared on large scale and soluble in acetonitrile.<sup>26</sup> In addition, the product is readily modified in subsequent transformations, a necessity for a building block to act as a scaffold. Acrylonitrile was chosen as the initial somophile due to its potential for subsequent derivatization.

To perform the flow reactions, we used an in-house constructed flow reactor,<sup>27,28</sup> equipped with 500 W input power of blue (460 nm) LEDs (Figure 1 and Figure 2). Perfluoroalkoxy (PFA) tubing is wound around a water-cooled copper core and provides an internal reactor volume of about 20 mL ( $\varnothing$  0.8 mm) along which the reaction mixture could be irradiated.

To prevent overheating and thermal side reactions, also the LEDs were water-cooled, maintaining a consistent temperature within the reactor. A continuous syringe pump offered precise flow control and pumps the reaction mixture through the PFA tubing at a constant rate. Behind the pump, a sample loop has been installed, which was used to inject small volume samples for conditions screening, bypassing the internal volume of the pump to prevent sample dilution.

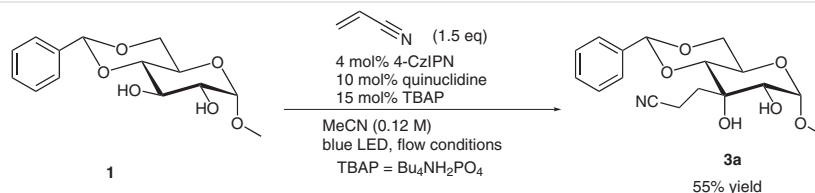
The study commenced by translating the reaction system from our established batch conditions<sup>7</sup> to the continuous flow setup, after which several parameters were modified to optimize product yield.

**Figure 1** Schematic of the flow reactor**Figure 2** Reactor setup, water-cooled internals

It is crucial that over the course of the reaction the mixture stays homogeneous, as in-line crystallization causes the flow system to fail due to channel blockage.<sup>29</sup> Crystallization can take place both in the tubing and in the pump, imposing restrictions on the maximum concentration at which the reaction can be carried out.

Experiments to maximize the conversion were carried out varying several parameters. We observed that when the light output was reduced, the conversion dropped significantly, in an almost linear fashion.<sup>30</sup> Subsequently, the reaction was performed at different substrate concentrations. It was found that there was no significant change in conversion when the concentration of the substrate was either increased or decreased. We settled on a substrate concentration of 0.12 M, well below the maximum solubility in order to prevent precipitation.

Upon changing the iridium catalyst for 4-CzIPN in our batch flow system, similar conversions were observed albeit at a somewhat higher catalyst loading (Scheme 4). This is analogous to Wendlandt's observations in the epimerization reaction.<sup>15</sup> Although no significant change in conversion was observed when the catalyst loading was varied between 2.5 mol% and 4 mol%, the latter was chosen for larger



**Scheme 4** Photoalkylation of methyl 4,6-O-benzylidene- $\alpha$ -D-glucopyranoside in flow

scale reactions in order to have flexibility in the residence time. The apolar nature of 4-CzIPN allows it to be removed easily from the reaction mixture by chromatography.

Although we initially started with a 25 mol% loading of tetrabutylammonium dihydrogen phosphate (TBAP), reducing the loading of the TBAP cocatalyst to 15 mol% did not have a pronounced effect on the overall conversion and reduced the risk of precipitation. Increasing the equivalency of the somophile acrylonitrile above 1.5 did not have a positive result. Instead, unreacted or polymerized somophile was recovered after the reaction.

Purification of the reaction mixtures is rather straightforward. Dependent on the somophile used, the excess was evaporated under reduced atmosphere, together with the solvent. The TBAP and the quinuclidine were removed by aqueous wash, whilst the remaining 4-CzIPN and its decomposition products were removed by separation by column chromatography. With commercial equipment, it would be possible to carry out liquid–liquid extraction directly in-line, further simplifying purification.<sup>31</sup>

When subjected to these optimized conditions, with a residence time of  $T_r = 20$  minutes, **1** could be alkylated on 1-gram scale in 55% isolated yield (**3a**). Increasing the residence time did not result in a significantly higher conversion. The impurity profile of the crude suggested that some decomposition of the benzylidene acetal took place, although a clear side product could not be isolated. It is not unlikely that the C–H bond of the acetal can also be activated in this reaction. The use of an alternative protecting

group without such a hydrogen, for instance a di-*tert*-butylsilyl group, may avoid this problem, at the expense of increased cost.

In addition to acrylonitrile, several other somophiles were used in the alkylation reaction, with mixed results (Figure 3). Notably, the required residence time for these somophiles was significantly larger than that of acrylonitrile (0.25 mL/min vs 1 mL/min). Reactions with alkenes such as phenyl vinyl sulfone and diethyl vinyl phosphonate performed well, providing **3b** and **3c**, respectively. In an attempt to increase the scope, we also studied styrene derivatives and vinylpyridine, although these were expected to be very weak somophiles. We were pleased to see that *m*-chlorostyrene and in particular 2-vinylpyridine do act as somophiles in this reaction, giving **3e** and **3f**, respectively. Although the yields are somewhat unsatisfactory still, in particular for the preparation of pharmaceutical scaffolds this broadening of the scope is significant. Bromostyrenes were studied as well, but decomposed under these conditions.

To confirm the value of performing these reactions in flow, the alkylation of **1** with acrylonitrile was carried out on 40-gram scale. As increasing the residence time with this somophile had only negligible effect on product yield, a residence time  $T_r = 20$  minutes was chosen. After purification, 45% (21.4 g) of **3a** was isolated.

In summary, by performing the established photoalkylation in flow, it has been demonstrated that this reaction can be carried out on a multigram scale. The replacement of the iridium photocatalyst with an organo-photocatalyst al-

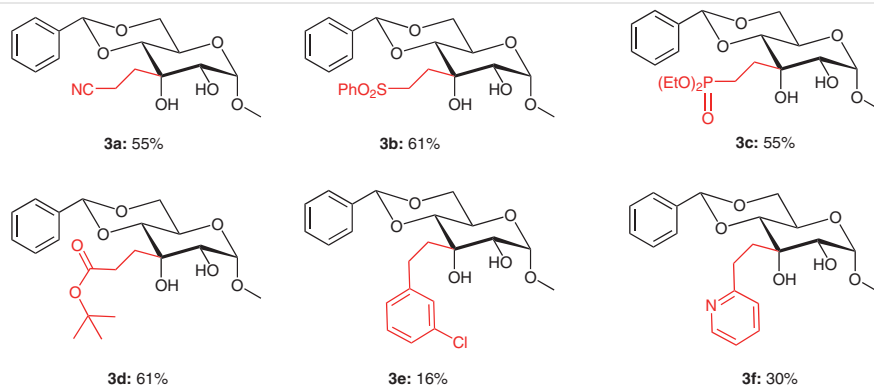


**Figure 3** Somophile scope of gram-scale flow reactions



lows the reaction to be carried out cost-effectively, offering large-scale production potential. Reactions with several somophiles were carried out on gram scale and a representative example was scaled to 21 g of product. The set of applicable somophiles has been expanded with 3-chlorostyrene and 2-vinylpyridine, which makes the products more interesting from a pharmaceutical point of view. We are currently focused on the follow-up chemistry of these compounds. In the future, it would be interesting to investigate the reaction with the recently reported HAT agents, as well as different carbohydrate substrates.

All reagents were purchased from commercial sources. Somophiles were distilled prior to use, with exception of those that are heat-sensitive. Reaction mixtures were pumped through the flow reactor by means of a Syrris Asia syringe pump. NMR spectra were recorded on a Bruker Avance NEO (400 MHz) spectrometer at room temperature. High-resolution mass spectrometry (HRMS) was carried out on a Thermo Fisher Scientific LTQ Orbitrap XL (FTMS) instrument. IR spectra were recorded on a Thermo Fisher Scientific Nicolet 380 FT-IR spectrometer.

#### Alkylation of Methyl 4,6-O-Benzylidene- $\alpha$ -D-glucopyranoside (1) in Flow; General Procedure

To a 50-mL round-bottom flask with stir bar was added methyl 4,6-O-benzylidene- $\alpha$ -D-glucopyranoside (**1**; 1.00 g, 3.54 mmol), 4-CzIPN (112 mg, 142  $\mu$ mol, 4 mol%), quinuclidine (40 mg, 0.36 mmol, 0.1 equiv) and tetrabutylammonium dihydrogen phosphate (TBAP; 180 mg, 530  $\mu$ mol, 0.15 equiv). The flask was subsequently capped with a septum and purged with nitrogen. Freshly degassed acetonitrile (28 mL) was added and the mixture was stirred until dissolution. Subsequently, the somophile (1.5 equiv) was added by injection via the septum, after which the solution was stirred for an additional 5 min. The mixture was subsequently pumped through a 20-mL flow system ( $T_r$  = 80 min) under irradiation of blue light by automated syringe and collected in amber glassware. After solvent evaporation, the remaining material was dissolved in DCM (25 mL) and washed with water and brine (10 mL each, to remove the TBAP). After solvent evaporation, the residue was purified by column chromatography, providing the desired product.

#### 3a by Large-Scale Alkylation of Methyl 4,6-O-Benzylidene- $\alpha$ -D-glucopyranoside (1) with Acrylonitrile in Flow

To a 2-L round-bottom flask with stir bar was added methyl 4,6-O-benzylidene- $\alpha$ -D-glucopyranoside (**1**; 40.0 g, 142 mmol), 4-CzIPN (4.45 g, 5.6 mmol, 4 mol%), quinuclidine (1.58 g, 14.2 mmol, 0.1 equiv) and TBAP (7.21 g, 21.3 mmol, 0.15 equiv). The flask was capped with a septum and purged with nitrogen. Freshly degassed acetonitrile (1.4 L) was added by injection via the septum, after which the solution was stirred until homogeneous. Acrylonitrile (14.1 mL, 213 mmol, 1.5 equiv) was then added through the septum, after which the mixture was pumped through a 20-mL flow system ( $T_r$  = 20 min) under irradiation of blue light by automated syringe and collected in amber glassware. After solvent evaporation, the remaining material was dissolved in EtOAc and washed with water and brine (200 mL each, TBAP removal). After solvent evaporation, the residue was purified by column chromatography, affording **3a** (21.4 g) in 45% yield.

#### 3a by Reaction of 1 with Acrylonitrile

White solid; yield: 711 mg (55%);  $R_f$  = 0.2 (EtOAc/heptane, 50:50).

IR: 3390, 2998, 2941, 2867, 2248, 1070, 1038, 1014, 997  $\text{cm}^{-1}$ .

$^1\text{H}$  NMR (400 MHz, DMSO- $d_6$ ):  $\delta$  = 7.45 (dq,  $J$  = 6.5, 2.3 Hz, 2 H), 7.42–7.35 (m, 3 H), 5.61 (s, 1 H), 4.86 (d,  $J$  = 9.4 Hz, 1 H), 4.62 (d,  $J$  = 4.0 Hz, 1 H), 4.25 (dd,  $J$  = 10.1, 5.2 Hz, 1 H), 4.17 (s, 1 H), 3.94 (td,  $J$  = 10.0, 5.1 Hz, 1 H), 3.67 (t,  $J$  = 10.3 Hz, 1 H), 3.50 (dt,  $J$  = 9.3, 2.1 Hz, 2 H), 3.33 (s, 3 H), 2.71–2.55 (m, 2 H), 1.98 (t,  $J$  = 8.0 Hz, 2 H).

$^{13}\text{C}$  NMR (101 MHz, DMSO- $d_6$ ):  $\delta$  = 138.26, 129.20, 128.50, 126.63, 121.75, 100.91, 100.60, 80.39, 72.70, 70.26, 68.80, 58.73, 55.86, 31.00, 12.29.

HRMS (ESI):  $m/z$  [ $M + \text{Na}$ ] $^+$  calcd for  $\text{C}_{17}\text{H}_{21}\text{NO}_6$ : 358.126; found: 358.125.

#### 3b by Reaction of 1 with Phenyl Vinyl Sulfone

Yellow solid; yield: 965 mg (61%);  $R_f$  = 0.35 (EtOAc/heptane, 60:40).

IR: 3478, 2933, 1466, 1286, 1143, 1067, 1044, 998, 745, 688  $\text{cm}^{-1}$ .

$^1\text{H}$  NMR (400 MHz,  $\text{CDCl}_3$ ):  $\delta$  = 7.85–7.79 (m, 2 H), 7.63–7.56 (m, 1 H), 7.50–7.44 (m, 2 H), 7.39 (dd,  $J$  = 6.9, 3.0 Hz, 2 H), 7.36–7.30 (m, 3 H), 5.50 (s, 1 H), 4.70 (d, 1 H), 4.32 (dd,  $J$  = 10.3, 5.0 Hz, 1 H), 3.93 (td,  $J$  = 9.9, 5.0 Hz, 1 H), 3.70 (t,  $J$  = 10.3 Hz, 1 H), 3.55–3.45 (m, 3 H), 3.44 (s, 3 H), 3.38 (d,  $J$  = 9.6 Hz, 1 H), 3.00 (s, 1 H), 2.56 (d,  $J$  = 11.9 Hz, 1 H), 2.31–2.13 (m, 2 H).

$^{13}\text{C}$  NMR (101 MHz,  $\text{CDCl}_3$ ):  $\delta$  = 139.15, 136.84, 133.54, 129.21, 129.17, 128.30, 127.99, 126.07, 101.73, 100.39, 81.65, 72.87, 71.32, 69.02, 58.72, 56.32, 51.84, 28.40.

HRMS (ESI):  $m/z$  [ $M + \text{Na}$ ] $^+$  calcd for  $\text{C}_{22}\text{H}_{26}\text{O}_8\text{S}$ : 473.124; found: 473.122.

#### 3c by Reaction of 1 with Diethyl Vinyl Phosphonate

Off-white solid; yield: 872 mg (55%);  $R_f$  = 0.15 (EtOAc/heptane, 50:50).

IR: 3395, 2934, 2863, 1984, 1067, 1039, 1022, 996, 958, 697  $\text{cm}^{-1}$ .

$^1\text{H}$  NMR (400 MHz,  $\text{CDCl}_3$ ):  $\delta$  = 7.54–7.40 (m, 2 H), 7.37–7.27 (m, 3 H), 5.49 (s, 1 H), 4.70 (dd,  $J$  = 3.8, 1.6 Hz, 1 H), 4.31 (ddd,  $J$  = 10.4, 5.1, 1.5 Hz, 1 H), 4.10–3.94 (m, 5 H), 3.70 (td,  $J$  = 10.3, 1.5 Hz, 1 H), 3.52 (d,  $J$  = 3.9 Hz, 1 H), 3.43 (s, 3 H), 3.36 (dd,  $J$  = 9.5, 1.6 Hz, 1 H), 2.16–1.96 (m, 4 H), 1.23 (apparent t,  $J$  = 7.0, 1.3 Hz, 6 H).

$^{13}\text{C}$  NMR (101 MHz,  $\text{CDCl}_3$ ):  $\delta$  = 137.17, 129.04, 128.18, 126.19, 101.76, 100.66, 80.75, 73.48, 73.34, 70.54, 69.18, 61.81, 61.75, 61.72, 61.66, 58.71, 56.24, 27.35, 27.31, 20.86, 19.46, 16.41, 16.35.

$^{31}\text{P}$  NMR (162 MHz,  $\text{CDCl}_3$ ):  $\delta$  = 34.41–32.42 (m).

HRMS (ESI):  $m/z$  [ $M - 2\text{H} + \text{Na}$ ] $^-$  calcd for  $\text{C}_{20}\text{H}_{31}\text{O}_9\text{P}$ : 467.144; found: 467.143.

#### 3d by Reaction of 1 with *tert*-Butyl Acrylate

White solid; yield: 885 mg (61%);  $R_f$  = 0.4 (EtOAc/heptane, 50:50).

IR: 3512, 3340, 2970, 2932, 2860, 1731, 1367, 1137, 1081, 1001  $\text{cm}^{-1}$ .

$^1\text{H}$  NMR (400 MHz,  $\text{CDCl}_3$ ):  $\delta$  = 7.51–7.42 (m, 2 H), 7.37–7.29 (m, 3 H), 5.52 (s, 1 H), 4.71 (d,  $J$  = 4.1 Hz, 1 H), 4.32 (dd,  $J$  = 10.3, 5.1 Hz, 1 H), 4.03 (td,  $J$  = 9.9, 5.0 Hz, 1 H), 3.71 (t,  $J$  = 10.3 Hz, 1 H), 3.50 (dd,  $J$  = 11.3, 4.1 Hz, 1 H), 3.45 (s, 3 H), 3.38 (d,  $J$  = 9.5 Hz, 1 H), 3.20 (s, 1 H), 2.84 (d,  $J$  = 11.3 Hz, 1 H), 2.60–2.40 (m, 2 H), 2.18–1.98 (m, 2 H), 1.38 (s, 9 H).

$^{13}\text{C}$  NMR (101 MHz,  $\text{CDCl}_3$ ):  $\delta$  = 173.71, 137.24, 129.05, 128.24, 126.23, 101.72, 100.52, 80.72, 80.53, 73.32, 70.83, 69.19, 58.65, 56.27, 30.49, 29.84, 28.07.

HRMS (ESI):  $m/z$   $[M + Na]^+$  calcd for  $C_{21}H_{30}O_8$ : 433.183; found: 433.182.

### 3e by Reaction of 1 with 3-Chlorostyrene

Yellow solid; yield: 245 mg (16%);  $R_f$  = 0.4 (EtOAc/heptane, 50:50).

IR: 3478, 2942, 2844, 1071, 1016, 987, 697  $cm^{-1}$ .

$^1H$  NMR (400 MHz,  $CDCl_3$ ):  $\delta$  = 7.55–7.50 (m, 2 H), 7.46–7.38 (m, 3 H), 7.26–7.17 (m, 3 H), 7.12 (dt,  $J$  = 7.2, 1.7 Hz, 1 H), 5.53 (s, 1 H), 4.83 (s, 1 H), 4.41 (dd,  $J$  = 10.3, 5.1 Hz, 1 H), 4.10 (td,  $J$  = 9.9, 5.0 Hz, 1 H), 3.77 (t,  $J$  = 10.3 Hz, 1 H), 3.67 (dd,  $J$  = 12.0, 4.1 Hz, 1 H), 3.54 (s, 3 H), 3.49 (d,  $J$  = 9.6 Hz, 1 H), 2.96 (s, 1 H), 2.86–2.77 (m, 2 H), 2.68 (d,  $J$  = 12.1 Hz, 1 H), 2.20–2.08 (m, 2 H).

$^{13}C$  NMR (101 MHz,  $CDCl_3$ ):  $\delta$  = 144.06, 137.14, 134.15, 129.66, 129.13, 128.52, 128.31, 126.58, 126.16, 126.11, 101.78, 100.75, 79.86, 74.21, 69.68, 69.22, 58.71, 56.38, 35.21, 30.22.

HRMS (ESI):  $m/z$   $[M + Na]^+$  calcd for  $C_{22}H_{25}ClO_6$ : 443.123; found: 443.122.

### 3f by Reaction of 1 with 2-Vinylpyridine

White solid; yield: 412 mg (30%);  $R_f$  = 0.2 (DCM/MeOH, 98:2).

IR: 2931, 1068, 1044, 995, 748, 698  $cm^{-1}$ .

$^1H$  NMR (400 MHz,  $CDCl_3$ ):  $\delta$  = 8.55–8.24 (m, 1 H), 7.61–7.46 (m, 1 H), 7.42–7.24 (m, 5 H), 7.12–7.01 (m, 2 H), 5.45 (s, 1 H), 4.73 (d,  $J$  = 4.1 Hz, 1 H), 4.31 (dd,  $J$  = 10.2, 5.1 Hz, 1 H), 4.14 (td,  $J$  = 9.9, 5.1 Hz, 1 H), 3.69 (t,  $J$  = 10.3 Hz, 1 H), 3.62 (d,  $J$  = 4.2 Hz, 1 H), 3.44 (d,  $J$  = 1.0 Hz, 3 H), 3.39 (d,  $J$  = 9.5 Hz, 1 H), 3.21–2.95 (m, 2 H), 2.38–2.10 (m, 2 H).

$^{13}C$  NMR (101 MHz,  $CDCl_3$ ):  $\delta$  = 161.87, 148.39, 137.51, 136.87, 128.86, 128.11, 126.23, 123.19, 121.17, 101.57, 100.78, 80.84, 73.50, 70.78, 69.31, 58.74, 56.25, 33.62, 32.30.

HRMS (ESI):  $m/z$   $[M + Na]^+$  calcd for  $C_{21}H_{25}NO_6$ : 410.157; found: 410.157.

## Conflict of Interest

The authors declare no conflict of interest.

## Funding Information

This work is supported by the Carbohydrate Competence Center's (CCC) 'CarboBased' program.

## Acknowledgment

C. H. M. van der Loo and T. van den Broek are acknowledged for their assistance in constructing the flow equipment.

## Supporting Information

Supporting information for this article is available online at <https://doi.org/10.1055/a-1840-5483>.

## References

- Jäger, M.; Minnaard, A. J. *Chem. Commun.* **2016**, 52, 656.
- Dimakos, V.; Taylor, M. S. *Chem. Rev.* **2018**, 118, 11457.
- Holmberg-Douglas, N.; Nicewicz, D. A. *Chem. Rev.* **2022**, 122, 1925.
- Cambié, D.; Bottecchia, C.; Straathof, N. J. W.; Hessel, V.; Noël, T. *Chem. Rev.* **2016**, 116, 10276.
- Suh, C. E.; Carder, H. M.; Wendlandt, A. E. *ACS Chem. Biol.* **2021**, 16, 1814.
- Jeffrey, J. L.; Terrett, J. A.; MacMillan, D. W. C. *Science* **2015**, 349, 1532.
- Wan, I. C.; Witte, M. D.; Minnaard, A. J. *Chem. Commun.* **2017**, 53, 4926.
- Dimakos, V.; Su, H. Y.; Garrett, G. E.; Taylor, M. S. *J. Am. Chem. Soc.* **2019**, 141, 5149.
- Sakai, K.; Oisaki, K.; Kanai, M. *Synthesis* **2020**, 52, 2171.
- Sakai, K.; Oisaki, K.; Kanai, M. *Adv. Synth. Catal.* **2020**, 362, 337.
- Gorelik, D. J.; Turner, J. A.; Virk, T. S.; Foucher, D. A.; Taylor, M. S. *Org. Lett.* **2021**, 23, 5180.
- Li, Y.; Miyamoto, S.; Torigoe, T.; Kuninobu, Y. *Org. Biomol. Chem.* **2021**, 19, 3124.
- Xiao, W.; Wang, X.; Liu, R.; Wu, J. *Chin. Chem. Lett.* **2021**, 32, 1847.
- Matsumoto, A.; Yamamoto, M.; Maruoka, K. *ACS Catal.* **2022**, 12, 2045.
- Wang, Y.; Carder, H. M.; Wendlandt, A. E. *Nature* **2020**, 578, 403.
- Zhang, Y. A.; Gu, X.; Wendlandt, A. E. *J. Am. Chem. Soc.* **2022**, 144, 599.
- Gorelik, D. J.; Dimakos, V.; Adrianov, T.; Taylor, M. S. *Chem. Commun.* **2021**, 57, 12135.
- Dimakos, V.; Gorelik, D.; Su, H. Y.; Garrett, G. E.; Hughes, G.; Shibayama, H.; Taylor, M. S. *Chem. Sci.* **2020**, 11, 1531.
- Turner, J. A.; Rosano, N.; Gorelik, D. J.; Taylor, M. S. *ACS Catal.* **2021**, 11, 11171.
- Carder, H. M.; Suh, C. E.; Wendlandt, A. E. *J. Am. Chem. Soc.* **2021**, 143, 13798.
- Shin, N. Y.; Ryss, J. M.; Zhang, X.; Miller, S. J.; Knowles, R. R. *Science* **2019**, 366, 364.
- Donnelly, K.; Baumann, M. J. *Flow Chem.* **2021**, 11, 223.
- Engle, S.; Kirkner, T. R.; Kelly, C. B. *Org. Synth.* **2019**, 96, 455.
- Shang, T. Y.; Lu, L. H.; Cao, Z.; Liu, Y.; He, W. M.; Yu, B. *Chem. Commun.* **2019**, 55, 5408.
- Bryden, M. A.; Zysman-Colman, E. *Chem. Soc. Rev.* **2021**, 50, 7587.
- Demchenko, A. V.; Pornsuriyasak, P.; De Meo, C. J. *Chem. Educ.* **2006**, 83, 782.
- Laudadio, G.; Noël, T. *Photochemical transformations in continuous-flow reactors*, In *Flow Chemistry – Applications*, Vol. 2; Darvas, F.; Dormán, G.; Hessel, V.; Ley, S. V., Ed.; De Gruyter: Berlin/Boston, **2021**, 1–30.
- Note: Both the LED chips and water-cooling are available at minimal cost online, making the entire reactor under \$500 (pump excluded).
- Hartman, R. L. *Org. Process Res. Dev.* **2012**, 16, 870.
- Wan, T.; Wen, Z.; Laudadio, G.; Noël, T. *ACS Cent. Sci.* **2022**, 8, 51.
- Buglioni, L.; Raymenants, F.; Slattery, A.; Noël, T. *Chem. Rev.* **2022**, 122, 2752.